Supporting Information

Exploratory studies of a multidimensionally talented Simple Mn^{II}-based porous network : Selective "turn-on" recognition @ Cysteine over homocysteine with an indication of cystinuria and renal dysfunction

Sourav Bej[ab], Abhijit Hazra[ab], Riyanka Das[ab], Sourav Kr. Saha[ac], Monserrat Corbella[d] and Priyabrata Banerjee[ab]*

a. Surface Engineering & Tribology Group, CSIR-Central Mechanical Engineering Research Institute, Mahatma Gandhi Avenue, Durgapur, 713209, India.

E-mail: pr_banerjee@cmeri.res.in, priyabrata_banerjee@yahoo.co.in; Web: www.cmeri.res.in, www.priyabratabanerjee.in; Tel: +91-9433814081

b. Academy of Scientific and Innovative Research (AcSIR), AcSIR Headquarters CSIR-HRDC Campus, Postal Staff College Area, Sector 19, Kamla Nehru Nagar, Ghaziabad – 201002, Uttar Pradesh, India

c. Present address: Faculty of Engineering, Hokkaido University, Kita-13, Nishi-8, Kita-ku, Sapporo, Hokkaido 060-8628, Japan

d. Department of Inorganic Chemistry, University of Barcelona, Barcelona, Spain.

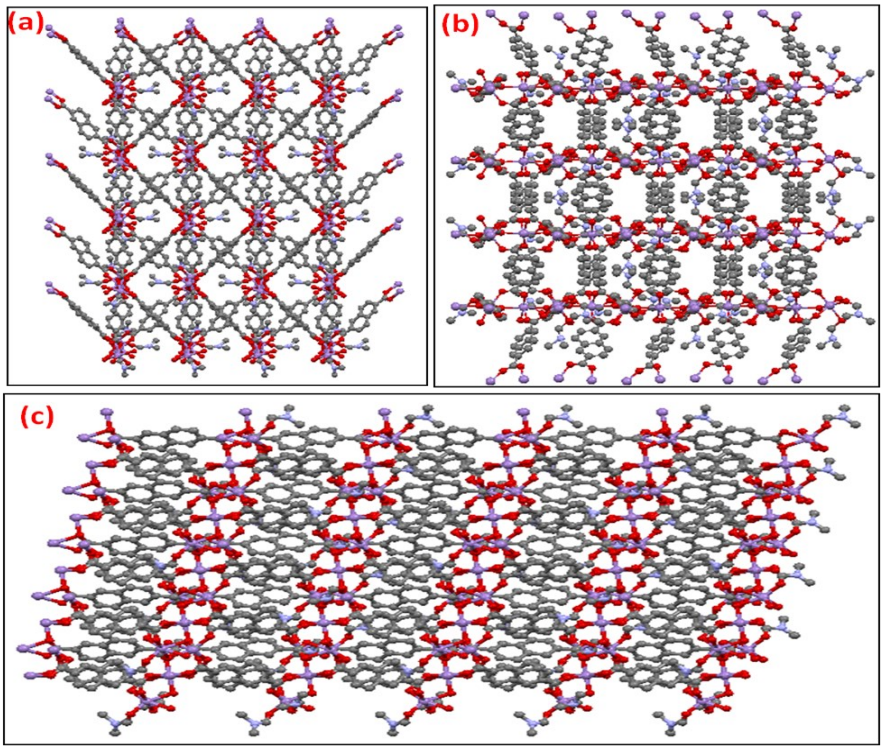

Fig. S1 The propagation of the 3D network of **PCP-1** along the view point of (a) *a*-, (b) *b*- and (c) *c*-axis.

PXRD

The powder X-ray diffraction (PXRD) patterns were measured using a Bruker AXS (D8)PXRD instrument.The crystallinity of the **PCP-1** was confirmed by low angle (in the range of 5 to 50 2θ value with the scan rate 0.5) PXRD analysis. PXRD patterns of the MOF, **PCP-1** matches well with the simulated PXRD pattern of **PCP-1**, indicating that the topology is retained and thus all members are isostructural.

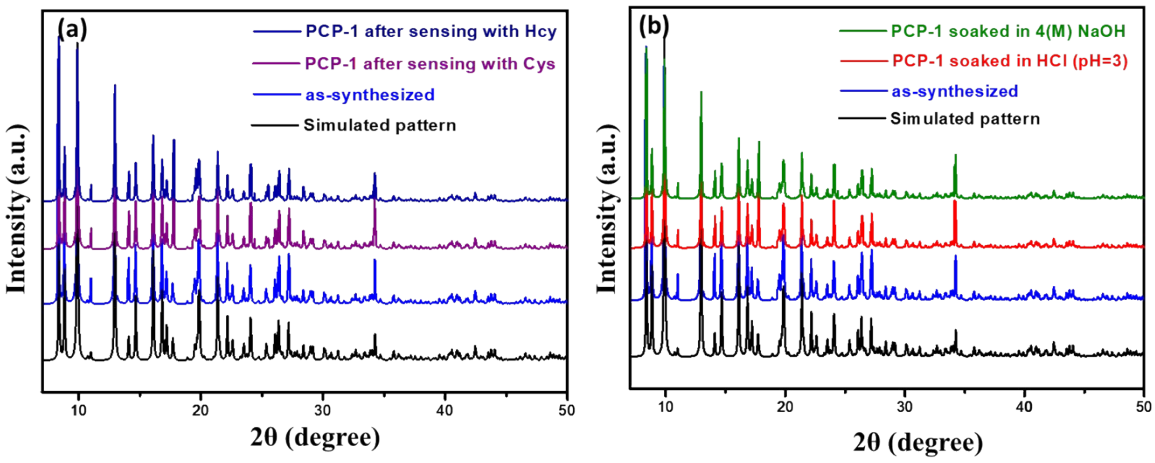

Fig. S2 (a) Experimental and simulated PXRD patterns of the as-synthesised MOF (**PCP-1**) along with its stability after sensing of biothiols **(b)** Stability of the **PCP-1** in different harsh conditions

Thermogravimetric analysis and framework rigidity

To characterize the thermal stability and thermal behaviour of **PCP-1**, Thermogravimetric Analysis (TGA) was carried out. TGA was conducted in nitrogen atmosphere from 0^0C to 800^0C with a heating rate of 5^0C/min. The results obtained from TGA analysis was depicted in **Figure S3**. It was observed that a mass loss of ~ 26.8 % till ~275 ^{0}C corresponding to the loss of the encapsulated guest solvent molecules, DMF (calcd. 26.58%). Thus, the desolvated MOF is quite stable upto ~275 ^{0}C. Beyond this, the MOF shows gradual decomposition.

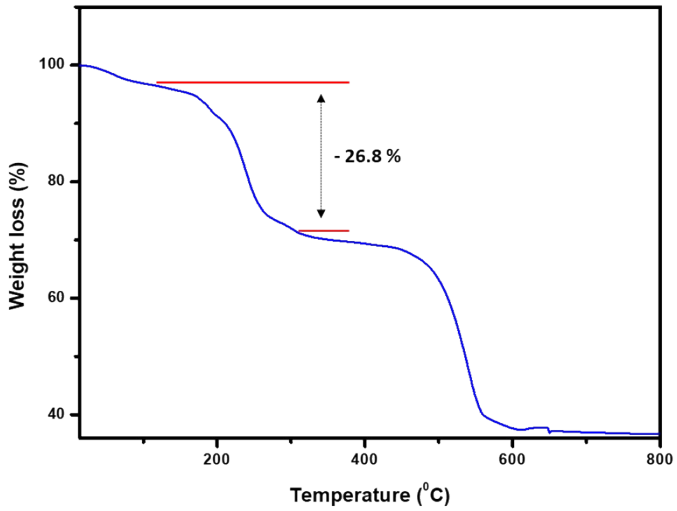

Fig. S3 TGA curve of MOF, **PCP-1** in nitrogen gas medium with a heating rate of 5^0C/min.

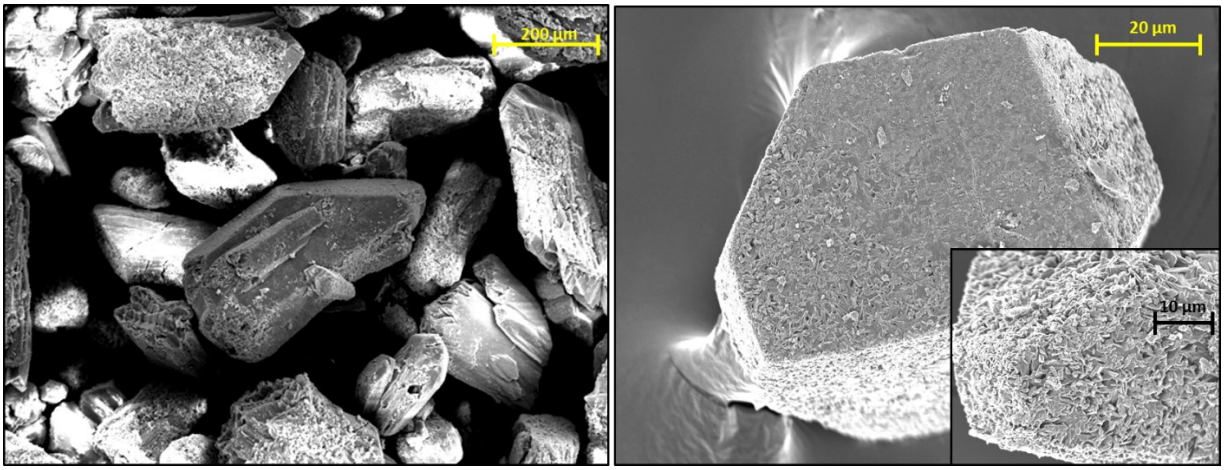

Fig. S4 FESEM images of MOF, **PCP-1** prepared by conventional solvothermal method.

HRTEM analysis:

High resolution transmission electron microscopy (HRTEM) **(**FEI, TF30, ST) was operated at 300 kV. The TF30 microscope was equipped with high-angle annular dark field (HAADF) detector (Fischione, model: 3000) and a scanning unit. Energy-filtered TEM (EFTEM) studies were accomplished using a post column imaging filter (Quantum SE, Model 963) from Gatan Inc.

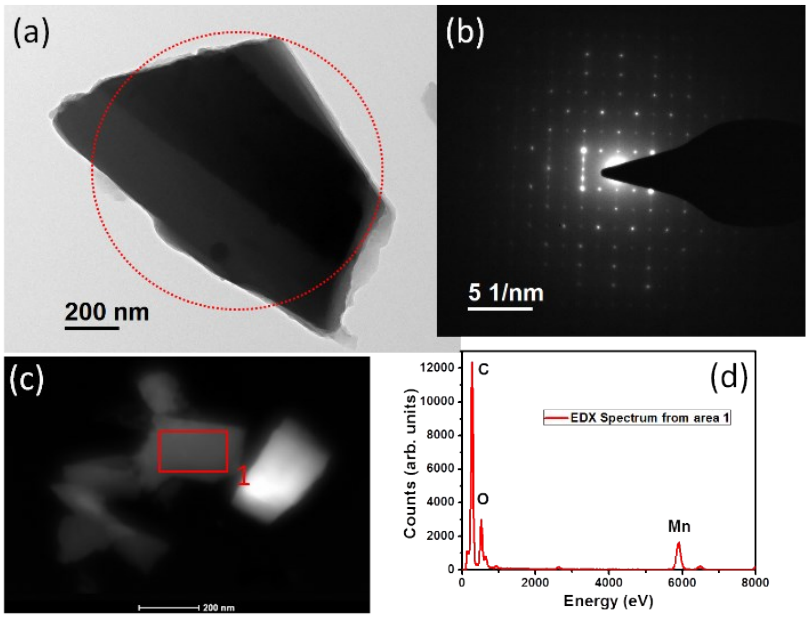

Fig. S5 (a) TEM image of MOF, **PCP-1**, (b) Electron diffraction pattern of the analysed porous material (c) STEM-HAADF image and (d) EDX spectrum taken from the region marked by 1

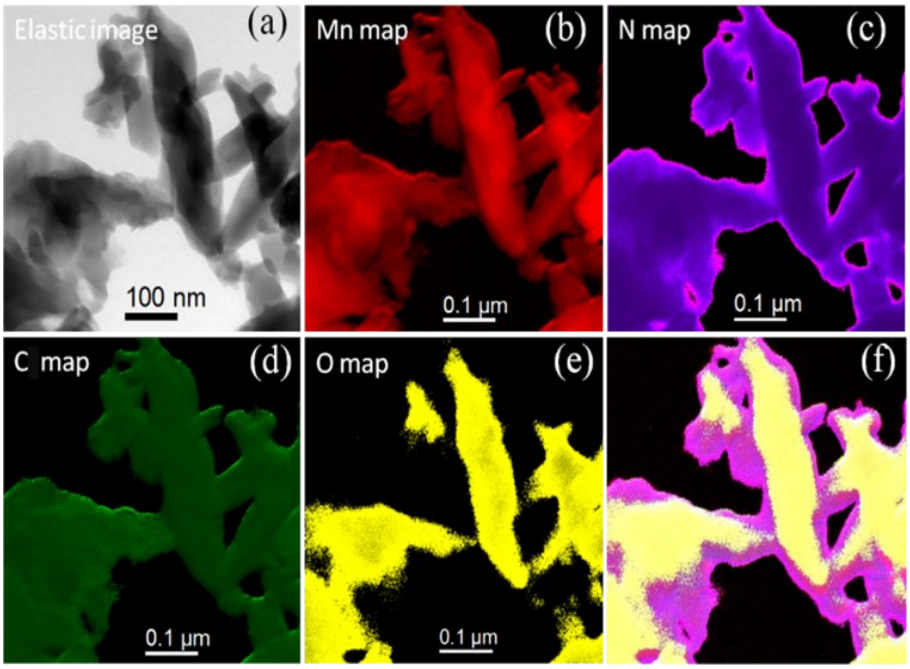

Fig. S6 EFTEM images of **PCP-1**. (a) elastic (zero-loss) image, (b) chemical map of Mn (red), (c) chemical map of N (blue), (d) chemical map of C (green), (e) chemical map of O (yellow) and (f) composite map.

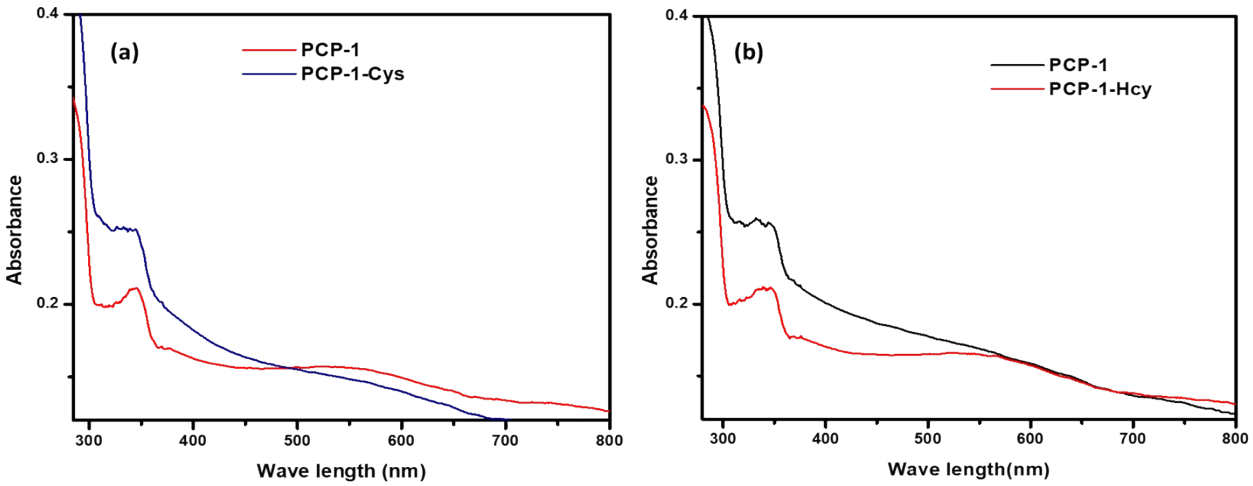

Fig. S7 (a) Absorption spectra of PCP-1 & PCP-1+Cys (b) Absorption spectra of PCP-1 & PCP-1+Hcy

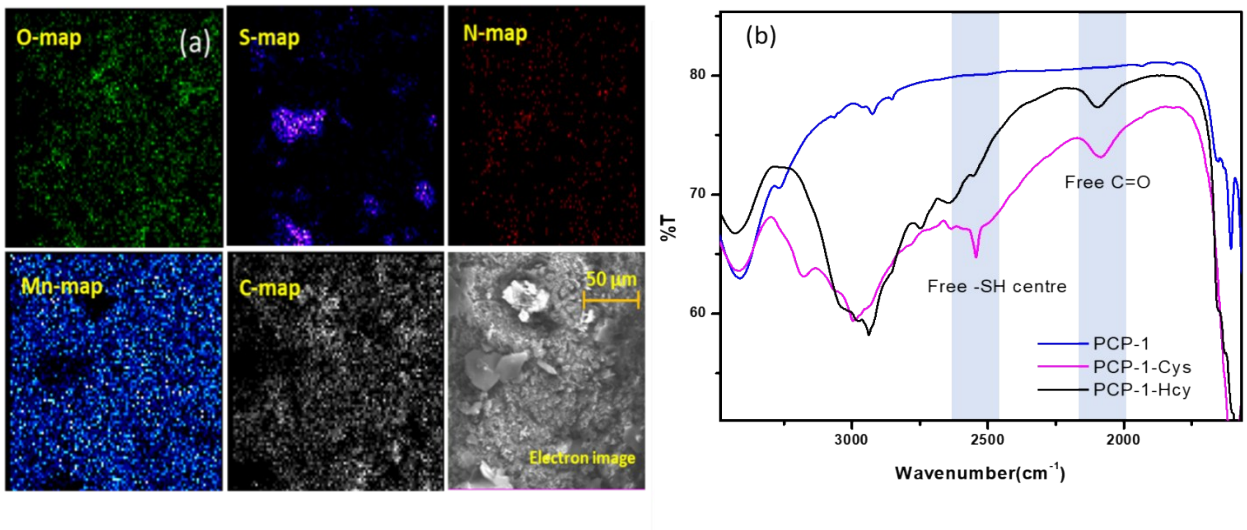

Fig. S8 (a) EDX mapping images of the Oxygen, Sulphur, Nitrogen, Manganese, Carbon atoms of **PCP-1** after interaction with biothiol (b) FTIR spectra of **PCP-1** after interacting with Biothiols

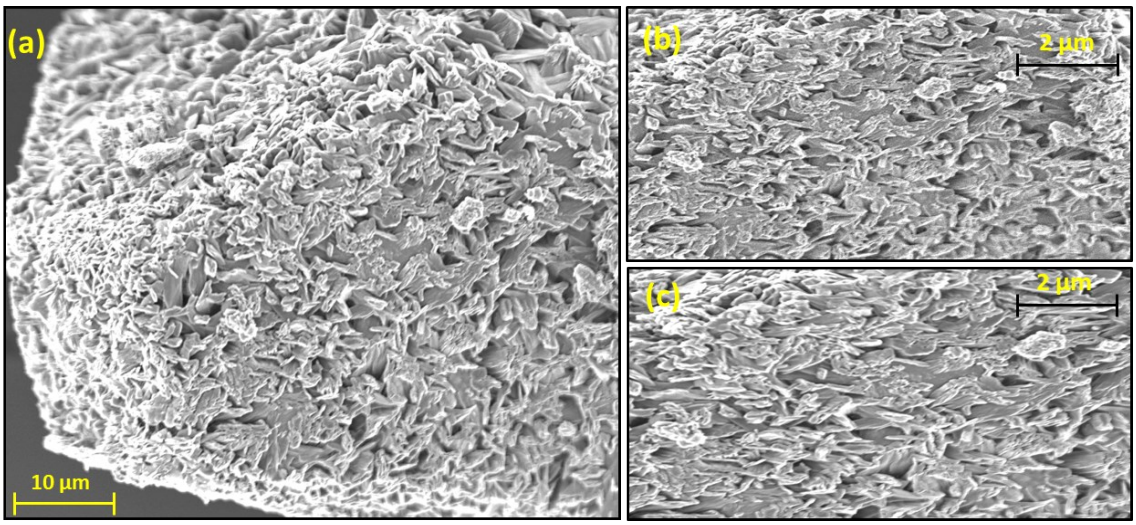

Fig. S9FESEM images of **PCP-1** (a) before interaction with biothiols (b) & (c) after interaction with Cys & Hcy respectively

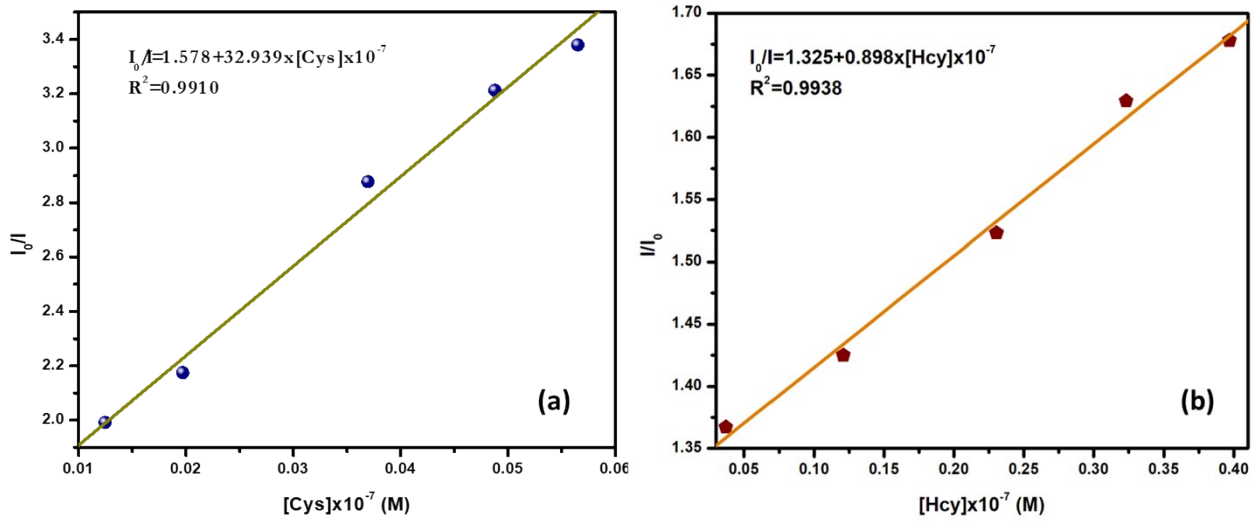

Fig. S10 Plot of (I_0/I) vs concentration of (a) Cysteine & (b) Homocysteine for the determination of limit of detection (LOD)

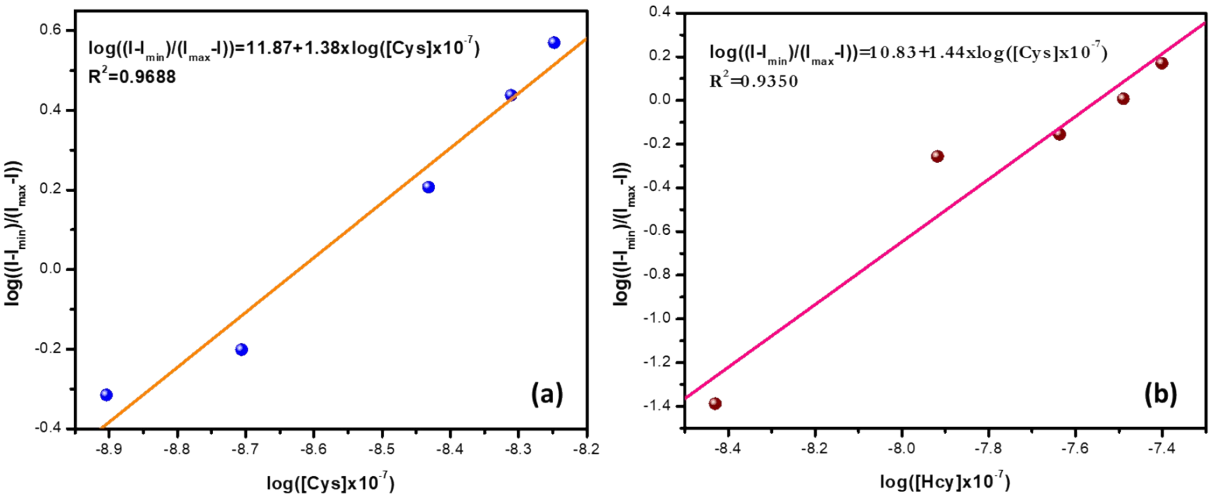

Fig. S11 Plot for the determination of association constant (K_a) by PCP-1 with biothiols (a) Cys & (b) Hcy

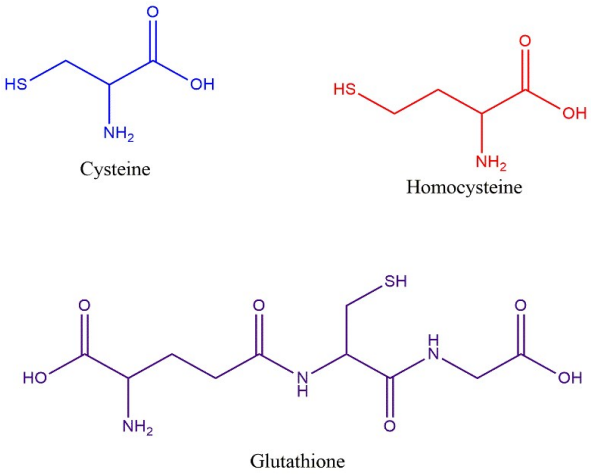

Fig. S12 Chemical diagram of biothiols.

Time-correlated single photon counting

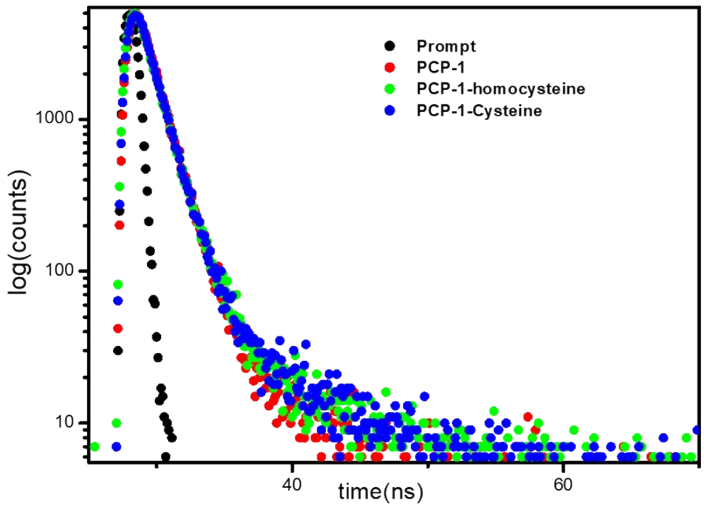

Fig. S13 Exited state life time parameters of **PCP-1 & PCP-1**+ biothiols

Table S1. UV-Vis spectral data of fluorophoric unit of **PCP-1** obtained from TD-DFT

Frequency	Oscillator strength
256.16103422	0.00091249
281.75365333	0.01500598
286.3905245	0.0012989
300.39761924	0.06764115
358.22464437	0.10245338

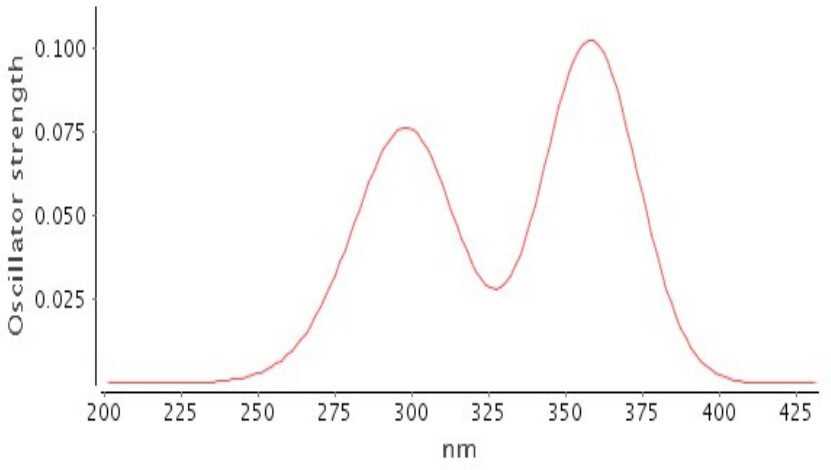

Fig. S14 UV-Vis spectrum of fluorophoric unit of **PCP-1** obtained from TD-DFT

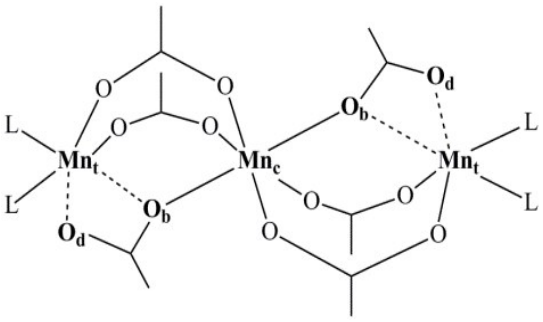

Fig. S15 Schematic structure of trinuclear complexes with $[Mn_3(\mu\text{-}RCOO)_6]$ core, showing the bridging mode of the caboxylato ligands.